Ascent and eruption at the Albuquerque Volcanoes: A physical volcanology perspective

L. S. Crumpler, 1999, pp. 221-233

in:

Albuquerque Geology, Pazzaglia, F. J.; Lucas, S. G.; [eds.], New Mexico Geological Society 50th Annual Fall Field Conference Guidebook, 448 p.

This page is intentionally left blank to maintain order of facing pages.

ASCENT AND ERUPTION AT THE ALBUQUERQUE VOLCANOES: A PHYSICAL VOLCANOLOGY PERSPECTIVE

L. S. CRUMPLER
New Mexico Museum of Natural History and Science, 1801 Mountain Road NW, Albuquerque, NM 87104

Abstract—The Albuquerque volcanic field (AVF) erupted 1 km^3 of lavas, averaging 1.5 m thick, and covering an area of 62 km^2. Eruptions occurred from a minimum of two en echelon dikes segmented from a much larger dike and relayed from a minimum depth of 12 km. The anomalously thick lava section exposed at Mesa Prieta at the southern end of the field is consistent with lavas ponded within the confines of an early graben resulting from near-surface deformation above the upward-propagating dike tip. Other graben and faults along the Ceja Mesa, if not tectonic, could be of similar dike-induced origin. Most of the apparent early sheet-like lava flows actually consist of numerous flow lobes, the margins of which are exposed as periodic breaks in the section along cliffs. In section, most of the flows bear systematic patterns of vesicle zonation interpreted to reflect steady growth of vesicles as solidification propagated inward from the upper and lower lava surfaces. Vesicle-free zones in some lava sections probably represent the effects of local lava flow inflation. Streamlined tumuli such as those distributed over the surface of earlier lavas formed when deflation left behind local pillars and tumuli that were subsequently engulfed by the overlying flow unit. The lengths of lava flows and morphology of lava flow channeling consistent with Gratz behavior enable estimation of effusion rates which range from 15 m^3 s^{-1} in the earlier phases of eruption to 0.3 m^3 s^{-1} during eruptions from the later stages at the principal cones. These are values typical of Hawaiian fissure eruptions. Unlike Hawaiian eruptions, the AVF was supplied by a single deep dike, and exhibited a monotonically decreasing volume rate with time. The morphology of pyroclastic deposits allows qualitative estimates of the relative contributions of gas content and volume flux. Initial events were dominated by high gas and high volume flux and optically thick fire fountains. As volume flux declined, eruptions evolved to higher relative gas contents, moderate explosive activity, and accumulation of coarse, poorly welded agglomerate and spatter, and rootless flows. The steady progression from early long lava flows to late short lava flows reflects a secular drop in magma driving pressure within the feeding dike. Driving pressure continued to fall until it was unable to overcome the yield strength of magmas and pyroclasts filling the upper part of the vents, even though fresh magmas remained within the lower parts of the feeding dike. Eventual accumulation of additional volatiles enabled development of pressures sufficient to exceed the yield strength, resulting in deformation, cracking, and local sector sliding of cone flanks. This was followed by late explosive destruction of portions of Vulcan cone, and an anomalously high volume rate (~100 m^3 s^{-1}) and shorted-lived effusion that flowed down the western flank where it temporarily ponded.

INTRODUCTION

The Albuquerque volcanic field (AVF) preserves characteristics, including small details of the eruptive processes, associated with the emplacement of basaltic volcanoes and lava flows. Many of these details are rare in any volcanic field, especially one situated near a major metropolitan area, and appear not to have been widely appreciated in the AVF, yet present valuable lessons in physical processes of volcanism. Over the past 20 years, knowledge of the processes of ascent and eruption, fissure and dike formation, lava flow emplacement, and basaltic pyroclastic phenomena have advanced as a result of continued research into the physics of volcanism. The purpose of this paper is to review some of the more general observations that may be made about the eruptions of the Albuquerque volcanoes from this new volcanological perspective; to discuss what may now be inferred about the events leading to their formation; and to highlight some potential directions for more detailed research. Many of the results must be considered speculative, and others in need of more expansive discussion than allowable in a paper of this limited magnitude. Nonetheless, the discussion leads to some appreciation of both the current development of volcanologic theory and the origin of an important feature of the local landscape.

Previous studies

The state of preservation of the AVF (Fig. 1A) is comparable to other basaltic volcanic features of the order of 10^5 years old elsewhere in New Mexico and may be considered morphologically youthful. Bachman and Mehnert (1978) report a K-Ar age of 0.19 ± 0.04 Ma, whereas recent ^{238}U-^{230}Th dating and magnetostratigraphy suggest an age closer to 0.14 Ma (Peale et al., 1996). The Cat Hills volcanoes, south of I-40 and visible to the west from I-25 in the vicinity of Los Lunas, are of a similar age (0.14 Ma: Kudo et al., 1977). The history of volcanism along the western side of the Rio Grande (the Ceja Mesa) and bordering areas extends back at least several million years before the present (Bachman and Mehnert, 1978). This includes isolated vents such as Los Lunas Volcano, Isleta Volcano, and Cerro Colorado, and other possibly buried volcanic centers detected in deep wells (J. W. Hawley, personal commun., 1998). The most important point is that the eruptions of the AVF are geologically young enough that the fundamental geological conditions from which the volcanism arose may still exist.

Previous mapping (Kelley, 1977; Kelley and Kudo, 1978) outlined one interpretation of the basic stratigraphic relationships of the field: a sequence of basaltic stratigraphic units in which the oldest flows are more widespread and are responsible for most of the field margins, particularly along the Petroglyph National Monument. Flows within subsequent stratigraphic units are progressively shorter and more restricted to the vicinity of the principal vents along the southern end of the fissure where the last activity appears to have occurred (Fig. 1B, C). Additional details of the eruptive sequence and the details of lava flows may be elaborated, including complications in the individual flow sequences, and local perched lava ponds, but the basic stratigraphy they outlined is useful as a working model of the erupted rock sequence. The following discussion will be fitted to this working stratigraphy for the sake of simplicity, while focusing on physical details that relate to the eruption process.

Basaltic lava flows of the AVF are olivine tholeiites (Aoki and Kudo, 1976; Kelley and Kudo, 1978; Baldridge, 1979; Zimmerman and Kudo, 1979; Kudo, 1982; Perry et al., 1987). They are compositionally more akin to Servilleta Formation basalts of the Taos Plateau (Baldridge, 1979) than other basalts of the central Rio Grande rift or tholeiites elsewhere within the Basin and Range Province. Samples from various points around the field are similar in major element composition, but slightly more mafic compositions characterize lavas erupted early on the southern end of the fissure and now exposed at Mesa Prieta (Baldridge, 1979). As pointed out later, the extensive "sheets" of basalt that form the lower unit in reality consist of numerous long flow lobes,

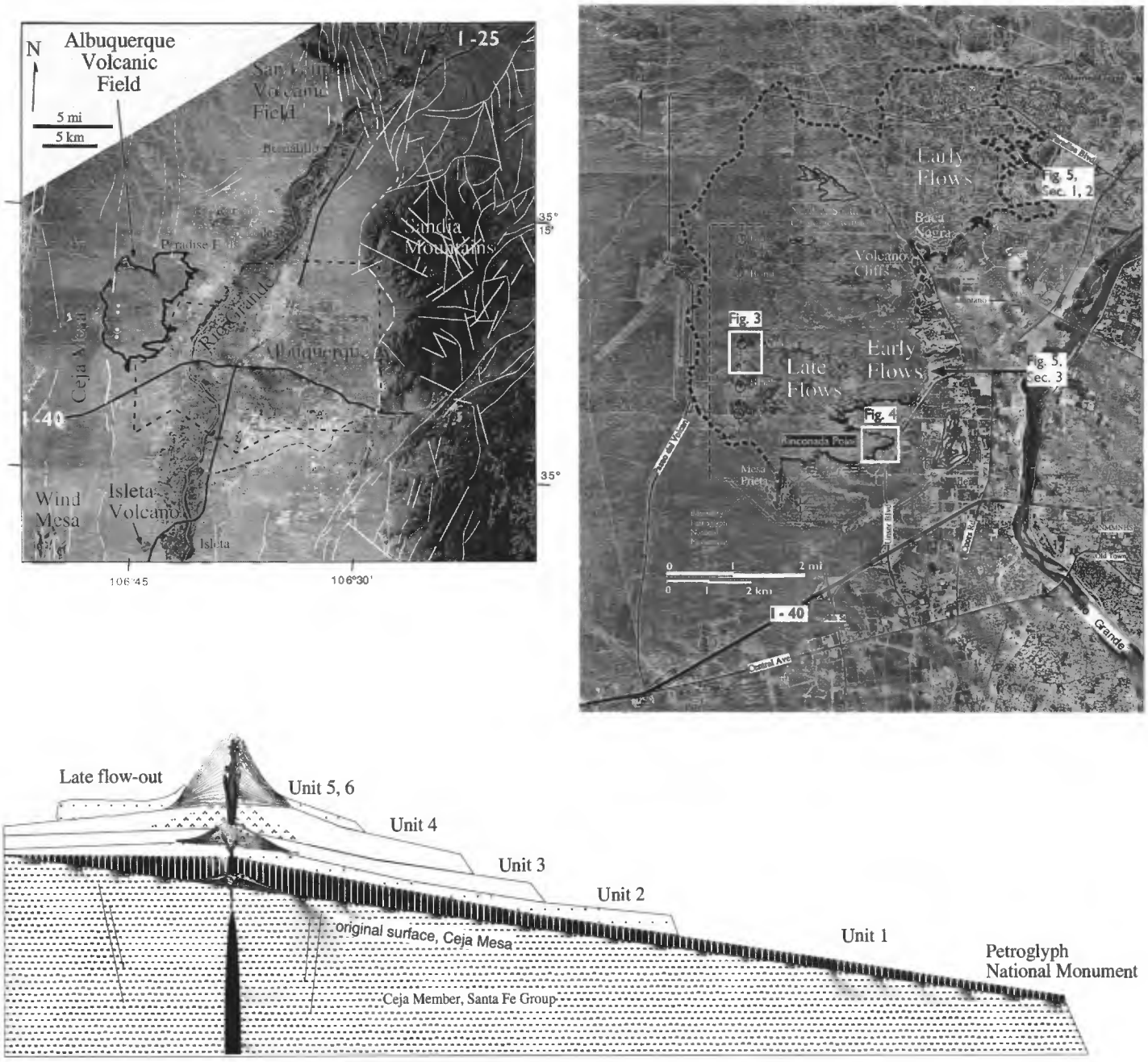

FIGURE 1. **A, (upper left)** Space shuttle image (STS040-0614-006) of the Albuquerque region showing the outline of the Albuquerque volcanic field in relation to the Rio Grande and regional physiographic and geographic features. White lines are faults from the tectonic map of Kelley (1977). Interstates I-40 and I-25 shown as black lines. The Albuquerque volcanic field fissure follows the trend of most faults on the Ceja Mesa. **B, (upper right)** Aerial photograph (1991) showing the outline of the field, location of the two primary fissure lines, location with respect to principal man-made features, and locations of Figures 3–5. Dark boulder-strewn slopes of the Petroglyph National Monument outline the margins of the field on the southeastern end. **C, (lower center)** Schematic east-west section showing the fundamental relationship among basaltic stratigraphic units assumed in this paper.

so it remains to be seen whether these inferences about temporal or spatial variations in composition are correct using a denser future sampling network, and based on the physical volcanology and a careful accounting of the pathways of individual channelized flows.

PHYSICAL CHARACTERISTICS

Eruptions occurred from a fissure 8 km long, as measured between the extreme southern and northern vents. The orientation of the fissure over the length of the three primary cones on the southern end (JA Cone, Black Cone, and Vulcan Cone) and two smaller cones on the northern end of the fissure (Bond Cone and Butte Cone) is N 1.5° E This parallels the orientation of the general western margin of the Albuquerque-Belen basin part of the Rio Grande rift. JA Cone, Black Cone, and Vulcan Cone, and Bond Cone and Butte Cone form two segmented (en echelon) fissures, each between 2 and 3 km in length, each striking approximately N 3° E (Fig. 2). Smaller vents north of Bond and Butte are aligned along an arc that trends somewhat more easterly, resulting in a northward extension of the fissure that curves slightly to the east.

The AVF fissure is located on a broad erosional surface sloping eastward ~1.5° toward the Rio Grande. As a result, most of the 62 km^2 area of lava flows lie to the east of the the fissure, and the eruptive fissure is offset toward the western edge. The upper surface of the field slopes somewhat more steeply in the vicinity of the principal vents,

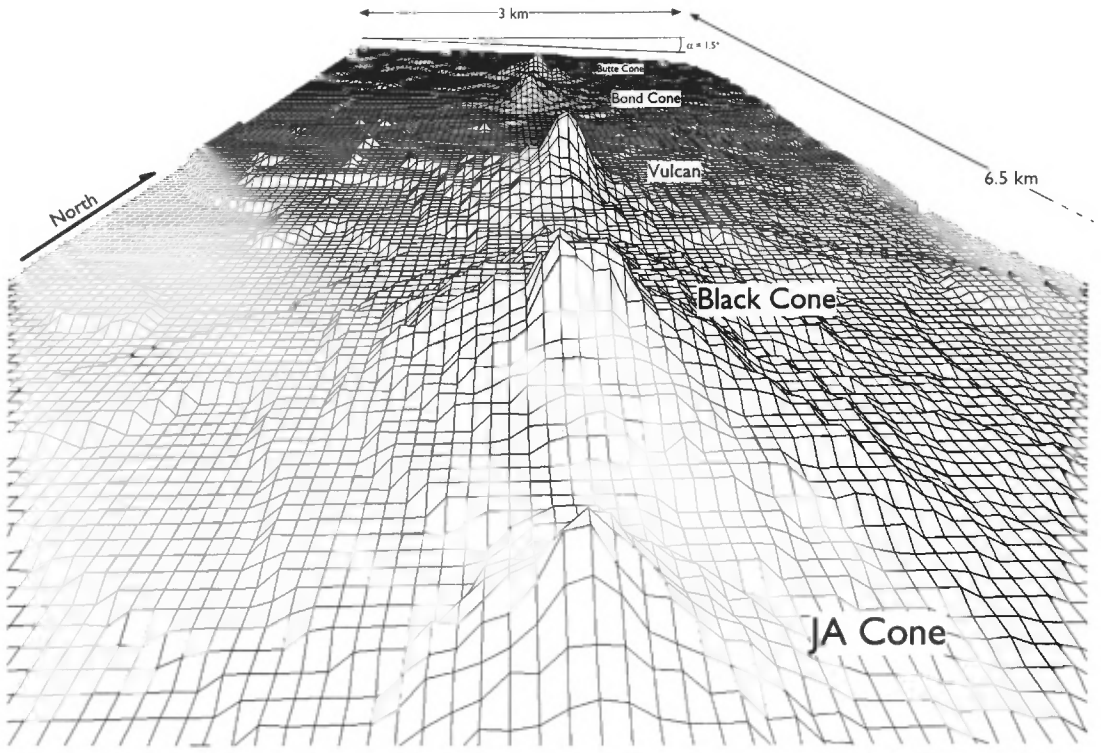

FIGURE 2. Digital terrain model of the Albuquerque volcanic-field fissure line constructed from 1:24,000-scale topographic data. View is directed N 1° E and shows the fissure as viewed from the southern end over the summit of JA Cone. The vertical scale is exaggerated ~1.5 times to highlight significant relief features. The en echelon offset between the southern and northern cones is clearly visible, as is their slightly differing strikes. The regional slope of the Ceja Mesa to the east is visible in the model horizon. A late flow forms a broad ridge extending westward from Vulcan, and a slightly smaller flow extends westward from Black Cone in the foreground.

attaining a maximum of 40° on the upper flanks of the largest cones and decreases to ~1° on the distal edges along the cliffs of the Petroglyph National Monument. Projecting this gradient from the cliffs westward beneath the volcanic materials, the lava section and associated pyroclastic materials near the fissure are estimated to attain a thickness of approximately 40 m near the source fissure. Lava flows exposed in section along the cliffs on the east are relatively thin, measuring from 1–2 m thick. Lengths of flows from the fissure to the cliffs are as much as 5–8 km in directions toward the Rio Grande and less than 2 km to the west onto the general surface of the Ceja Mesa. Using these values, and average relief along the fissure of 30 m, and assuming simple triangular sectional geometry for the bulk of the lava field, the volume of the AVF field as currently preserved is estimated at 1.1 km^3. A value of the order of 1 km^3 appears repeatedly in estimates of many basaltic flow fields in the Southwest (e.g., Wood and Kienle, 1990) and is an issue that bears future examination. It may reflect the constraints on magma driving pressures determined by recurring characteristics of the crustal rocks, regional tectonism, and geometry of feeding dikes, in each of these fields.

The fissure is less developed on the northern end, yet the most distal preserved lava flows occur there and in the vicinity of Paradise Hills. Throughout the eastern and southern margin, the basalt lava flows stand as dark mesas 50–60 m above the surrounding drainages. The modern drainages isolating the field are cut into sediments of the Ceja Member of the Santa Fe Formation (Kelley, 1977) and are probably reasonable models for the type of surface on which the lava flows were originally erupted. Whether lava reach was as far as the Rio Grande valley cannot be determined due to downcutting of the river since the eruptions. Given the thinness of the lava flows on their distal ends along the lava bluffs, it is likely that the total volume of the field prior to erosion was greater by only a small fraction.

Tectonic setting

The field lies on the western edge of the Albuquerque basin and near the central axis of the Rio Grande rift as defined structurally and on the basis of the east–west extent of Tertiary sediments. It is located on the relatively flat surface of the Ceja Mesa separating the Rio Grande on the east and Rio Puerco on the west (Kelley, 1977) and graded on sediments of the Santa Fe Formation. Initiation and ascent of magmas may have been facilitated beneath the center of the rift at the location of the AVF because the asthenosphere may be shallower there. Because faults are common throughout the Ceja Mesa (see Fig. 1A), once initiated, magma ascent would have been facilitated by the favorable stress environment in the crust.

The fissure alignment follows the orientation of most of the observable surface structures along this part of the basin and either derives from the pervasive faulting along the Ceja Mesa or is at least in part responsible for some of the faulting. The latter point is not an aggrandizement of the role of volcanism as a structural force, but acknowledges existing models of fracture propagation and crustal dilation over dikes which predict deformation in the near surface (Pollard, 1987; see later discussion below). On a line with the Volcanoes, the Nine Mile Hill fault of Kelley (1977) is down-thrown to the east and is interpreted to continue northward 1 km west of and parallel to the AVF fissure line. South of I-40, a parallel fault, down dropped on the west, continues parallel to the Nine Mile Hill fault, terminating just north of the latitude of Wind Mesa. Beginning near Wind Mesa, a series of down-to-the-west faults step westward where they displace basalts of the Wind Mesa field. Wind Mesa is bifurcated by a wide (1 km) graben. The surface of Ceja Mesa between the AVF and Wind Mesa also bears several peculiar closed basins that, although not associated with any mapped faults, may represent the eroded remains of additional graben-like displacements. Local variations in lava-flow thickness, described below, may indicate the presence of similar pre-eruption depressions or grabens.

Cones and vent structures

The AVF deposits are Hawaiian in style (e.g., Williams and

McBirney, 1979): long fissures, evidence for mild to strong fire fountaining, and subsidiary activity characterized by local ash and spatter accumulations near the vent areas. The latter stages of the eruptions were more Strombolian, in which bursts of dispersive pyroclastic activity occurred, scoria and ash were relatively more common, and lava fountains were small and sporadic.

The morphology of the principal cones is unusual compared with that of scoria ("cinder") cones common in most of the volcanic fields in the Southwest: (1) the cones are small, measuring between 30 and 150 m in basal width and 6–50 m high; typical, mature scoria cones average 0.9 km and 160 m, respectively (Wood 1980); (2), the cones are composites of ash, cinder, bombs, spatter, and significant volumes of rootless flows and fluid agglomerate, whereas most scoria cones contain proportionately greater volumes of brittle pyroclasts in which fluidal deposits are relatively minor and largely restricted to the interior slopes and crest of the summit craters; and (3) significant deformation occurred in several of the cones during the latter stages of eruption, particularly at JA, Black, and Vulcan (Kelley, 1982).

Vulcan, also known as 'J' Cone, is the largest and in many ways the most complex edifice. It is part of a north–south, elongated rise 350-m wide and 650-m long consisting of at least five edifices and structures here referred to as the Vulcan Group. These are situated on a broad elongate topographic relief, the Vulcan platform (Fig. 3). The visible outer layers of the steep cones in the Vulcan Group consist of a carapace of moderately-welded agglutinate and spatter forming, rough and knobby outcrops overlying fine to coarse, angular and poorly-welded cinder. The cone-like symmetry of Vulcan as viewed from the south belies the actual north–south elongation of the entire Vulcan Group along the local fissure orientation and complications brought about by various destructive explosive events. The steep, 150-m-wide conical portion of Vulcan-proper occupies the center of the Vulcan Group vent complex. The summit "crater" of Vulcan is a flat, 43-m-wide circular surface, tilted toward the west, formed when late lavas upwelled and filled an original summit crater. The edges of this crater may be mapped as a vertical discontinuity in agglomerates and cinders beneath an arch of welded spatter on the south rim. East of a north–south center-line drawn through the summit platform are bulbous outcrops of vesiculated and oxidized lava and scoria that squeezed up along a late throughgoing fissure. These may be the more visible parts of a late intrusion that resulted in deformation of the cone and its flanks (noted above and discussed in more detail later).

The summit crater-filling lava is covered with angular cinders and ash possibly deposited in part during a late crater-forming event that occurred between Vulcan and a smaller edifice, North Vulcan, to the immediate north. The resulting 90-m-wide crater opened an east–west breach between the two cones during the last, or very nearly last, eruptive activity, partially exposing the interiors of both Vulcan and North Vulcan. A 1–2-m-thick cap of lava filling the original summit crater of Vulcan is thus naturally sectioned by this crater, as are lavas filling a summit crater on North Vulcan. Within this exposed section there are several small reddish, equant, and vesicular bombs that fell into the still liquid lavas and settled to the base of the flows. This illustrates the concurrently explosive and effusive character typical of Hawaiian and Strombolian eruptions. It also illustrates one of the minor details and exciting little "stories" that are preserved in these cones.

Smaller vents in the Vulcan group, Baby Vulcan A and B, occur on the south and west flanks of the Vulcan platform and repeat many of the characteristics observed on Vulcan at a smaller scale. Each is 35–40 m in basal diameter and constructed of scoria overlain by late spatter. A filled summit crater 14-m wide on Baby Vulcan A is surrounded by a carapace of both outward-dipping spatter and agglutinate outcrops. Collapse of the upper part of the spatter carapace left inward-dipping

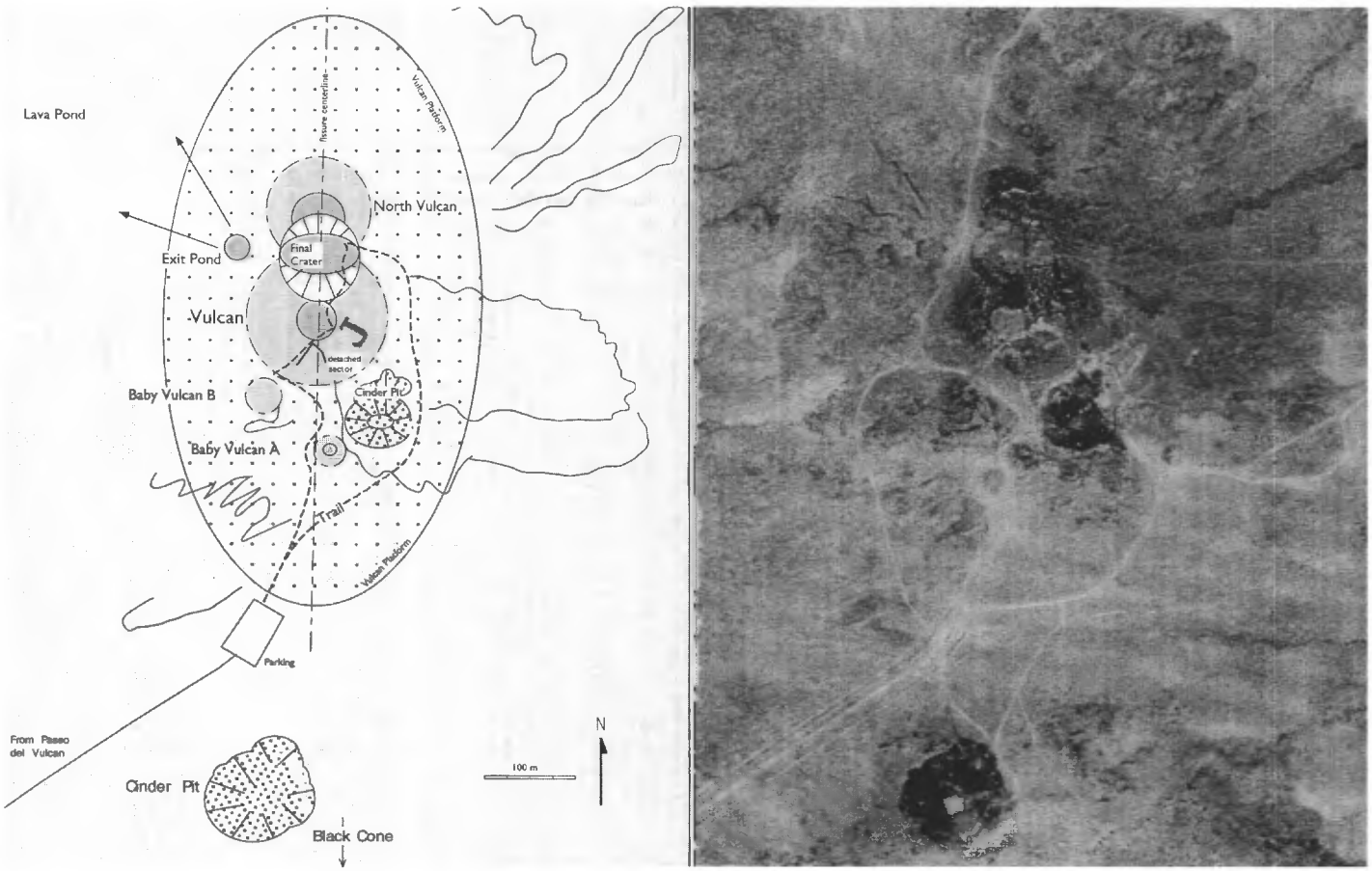

FIGURE 3. Schematic map of the principal characteristics of the Vulcan Group which is located on a broad elliptical rise (referred to as the Vulcan Platform in the text). The interior of the platform consists of earlier scoria and fragmental cinder and fountain-fed flows.

outcrops around the north margin. Abundant large gas pockets within the spatter probably resulted from gases trapped within the hot fluid clots.

A small-scale cinder pit operation conveniently exposes the pyroclastic deposits immediately underlying Vulcan. From these deposits it may be deduced that a large volume of scoria underlies the Vulcan Platform, and probably the other cones within the field. The scoria consists almost entirely of angular, fragmental, and brittle cinder, lapilli, and bombs, and a notable absence of fluid forms. Individual clasts were apparently cool upon landing, accumulation was slow and steady, and the fire fountain was relatively dispersed. This activity was in contrast to the conditions that prevailed during initial emplacement of the earlier widespread lava flow units in which the fountain must have been well-collimated; and contrasts with later activity when the flanks of the steep cones were coated with hot, fluid agglutinate.

Black Cone, south of Vulcan, is somewhat broader and its flanks less steep, consisting of radial lava-flow lobes. At its summit is a small pyroclastic cone composed of coarse agglutinate typical of the AVF cones in general. At the summit is a circular, filled crater. Several other late craters may be identified. The next to last, 40 m in diameter, is at the summit, and a final (somewhat larger, 50 m E–W and 60 m N–S) crater lies immediately to the northeast on the flank. As with Vulcan, this crater appears elongated along the general fissure trend and represents a late, explosive event.

JA Cone resembles Vulcan in that it is relatively steep. It too bears evidence of late deformation from swelling in the form of radial cracks from which some of the thin lava flows constituting a surrounding symmetric apron were erupted. Bond and Butte Cones at the northern end of the fissure are smaller cones consisting of coarse accumulated spatter and agglutinate otherwise similar to Vulcan. In contrast to the southern vents, the activity at these appears to have ceased earlier.

In addition to the five principal vents, there are up to 13 other subsidiary vents along the AVF fissure (Kelley, 1982), some as small as 10 m wide at the base and only a few meters high. Many of these smaller vent structures occur along the length of the AVF fissure frequently on the flanks or adjacent to the main edifices. The southernmost such vent lies 400 m south of the summit of JA Cone.

The deformation exposed on the flanks of several of the edifices is one of the more interesting characteristics from the standpoint of the dynamics of vent emplacement. It bears on the incompletely studied mechanics of magma emplacement in shallow conduits in the near-vent region. Limited deformation of cone flanks is not widely recognized in typical scoria cones. It may occur frequently, but is not preserved because of the easily deformed nature of loose scoria deposits, the relatively large size of most cones in relation to internal sources of inflation, and the corresponding difficulty in distinguishing such deformation where it does occur. In many larger scoria cones, late-stage swelling during increased volume flux of lava in the conduit leads ultimately to sector-like collapse and rafting outward of large segments of the cone flanks (Holmes, 1987). Breached, crescent-shaped, or horseshoe-shaped cones common in many volcanic fields (e.g., Crumpler et al., 1994, fig. 13) are the result. Other cones continue building after such large-scale deformation events take place. The AVF cones offer a rare opportunity to study this effect in its more incipient stages.

Several lines of evidence for cone inflation in the AVF cones exist. Radial cracks occur in the flanks where the carapace of spatter and lava has been isolated as sector-like blocks, suggesting internal expansion and cracking of the flanks. Prominent examples of grooved lavas expressed as slickenside-like grooves in outcrops on the upper slopes of the south flank of Vulcan imply that downslope sliding of the upper carapace of lava occurred while it was still plastic. The uppermost rootless flows draping the east flank of Vulcan are unusually steep, attaining a slope of 40°. The angle of repose on typical youthful cones is several degrees less than this, thus even flank flows are limited to values of the order of 35°. This is consistent with the flanks becoming steepened beyond their original stable repose, although steep repose can also characterize welded spatter.

One final point often noted by laymen when visiting the cones in winter, is the presence of "warm and steaming caves" (e.g., Simmons, 1982, p. 8). A prominent example of such a cave occurs on the east upper flank of Vulcan. These are unlikely to represent "volcanic heat," but are a result of the ice-box-like insulating properties of cinder. First, many of the caves like the one at Vulcan, which are often described as lava tubes, are in reality arches of welded spatter from which the underlying poorly-welded ash and cinder have been eroded, leaving behind cavities in the side of the cone. Many of these probably reflect the pervasive large-scale fracturing of the flanks during late-stage deformation and may form a loosely connected network of porous cinder and open cavities throughout the outer layers of the cones. Because of the excellent insulating properties of loose cinder, ambient air trapped within this network is likely maintained at the average annual temperature of Albuquerque (~13°C) and at relatively high dew points. On a cold winter day the air emerging from these "caves" appears "warm and moist" compared with exterior winter air that may be close to freezing and below the dew point of the escaping air mass. Second, the same caves are described as "cool and moist" when visited on the hottest summer days (although not usually noted because it is not nearly as exciting to report) because the emerging air is cooler and far moister than the ambient summer exterior air.

Pyroclastic deposits

Pyroclastic deposits are largely confined to the vicinity of the fissures, principally as cones and their underlying scoria deposits, although scattered clasts of cinder and ash occur throughout the surface of the lava flows in low-lying areas and welded into the basal and lateral rubble of individual flow lobes. Relatively little air-fall ash occurs beneath the few exposed basal sections of the flows, which is consistent with the minor ash cloud development and poor pyroclast dispersal in general associated with the Hawaiian style of the eruption (steady fire fountaining, volumetrically dominated by effusive eruptions). Pyroclastic materials are best exposed in the few cinder pits, an example occurring at the southeast base of Vulcan and illustrating the internal structure of the Vulcan Platform. In contrast to the pyroclasts on the visible exterior of the cones, fluidal forms are notably absent in these deposits and consist largely of strongly vesiculated and fragmented scoria and brittle cinder. The fragmental characteristics of the scoria deposits and their position high in the stratigraphic sequence of the fissure eruption are evidence of significant late-stage changes in gas and volume flux.

Lava flows

Pyroclastic cones are only the more prominent features of any basaltic eruption and typically constitute a small fraction (≤10%) of the erupted volume (Wood, 1980). This is true of the AVF. The general trend in large-scale morphology of the flows is such that the earliest lavas constitute the most voluminous and widespread units, and subsequent flows were increasingly shorter and narrower. Both from the detailed morphology of preserved surfaces and from the results of studies of lava vertical sections (Aubele et al., 1988), it is possible to characterize the AVF lavas as pahoehoe. As a general rule in the Southwest, lava flows on the order of 10^5 years old preserve the larger primary structures typical of most lavas. This includes flow margins, tumuli, pressure ridges, channels, and, locally, some smaller surface textures such as ropes, grooves, and lava ridges. The examples of these are scarce on the surfaces of the more widespread earlier AVF flows, largely because the more extensive flows are thin and probably had relatively low initial surface relief, and because of mantling of the low-lying areas with the pervasive West Mesa wind-blown deposits. Despite this, numerous examples of ropes, grooves, and deformed plastic shapes may be identified were the cover is typically thinned near the margins of the flows along cliffs and along drainages in the flow interior.

Surfaces of the lower and earlier stratigraphic units therefore appear to be relatively bland and uniform lava sheets at large scales, yet are actually complexly intertwined individual channelized flow lobes on the order of 100-m wide. The broadly pointed shape of Rinconada Point

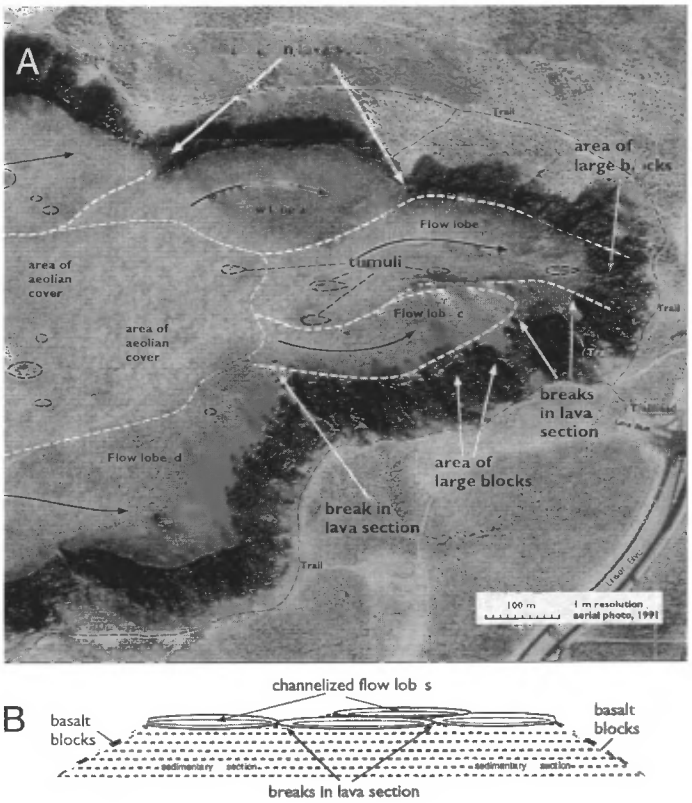

FIGURE 4. **A**, Aerial photograph of the Rinconada Point lava flows, one of the earlier stratigraphic units. Detailed mapping shows that the surface is not a single lava sheet, but a complex of individual flow lobes (a, b, c, d) of uncertain sequence of emplacement. Breaks in the lava section exposed around the margins of the mesa coincide with the margins of individual lobes. The largest debris blocks on the mesa slopes coincide with the thicker interior portions of each lobe. Unusual elongated and widely spaced tumuli (small, tapered ellipses) are oriented in the direction of flow. **B**, Schematic transverse (north-south) section of Rinconada Point showing variable thickness of basaltic cap related to multiple flow lobes.

is an example. In air photos it appears to be a single sheet of lava forming a lobe that covered and flowed down a broad paleo-valley. However, the margins of at least four individual channel-fed digitate flows and the remains of tumuli may be identified from geologic mapping of the surface (Fig. 4). The margins of the individual flows are frequently highlighted by zones of welded scoria and clinker. Some lobes appear to diverge from a central axial region as though they formed as large break-outs. Break-outs occur when the flow front attains its thermally-limited distance (discussed below) and the continued feeding of channeled lavas forces new lobes to develop and flow laterally around the preceding fronts. Along the exposed margins, lava sections alternately thin where the apparent margins of flow lobes are naturally sectioned and thicken where the interior of individual lobes are sectioned. Thus, the mesa edges consist of overlapping lens-shaped channels of lava. These patterns agree with the projected intersection of margins as mapped on the mesa surface and the areas of outcrop thinning seen on the mesa edges. The locations of thicker interior sections are also frequently highlighted in the mesa slopes by larger blocks eroded from the thicker and more wide-jointed flow centers. Frequently, these abundant and deeply varnished blocks are the sites of petroglyphs.

The tumuli are generally widely-spaced, less than 1 m in relief surrounded by scoria, and preserve some tilted and central structure resembling medial cracks. They are elongated down the gradient of the flow so that the highest and widest points are on the up-gradient side, and narrow down-gradient to merge with the surrounding surface in a shape that is "streamlined" in appearance. This form is not widely described from lava flow surfaces, but probably represents residual local relief on earlier flows, either remaining following deflation of originally inflated flows or developed as local pressure ridges. It is interpreted that, because they stood as barriers, subsequent flows moved around them, resulting in sculpted and streamlined shapes preserving the direction of flow.

In sections exposed along the eastern and southern margins of the field, the earliest lava stratigraphic units are thin, typically measuring from 1 to 2 m in thickness. Local sections up to 9 m in thickness (Fig. 5) occur where the flows were apparently channelized in narrow drainages. The channeling resulted in complex overlapping of short flow lobes. The lavas were fluid enough that in some places narrow lobes resembling pillow-lavas developed as small break-outs developed and flowed between pre-existing flow margins.

Where two or more flow units occur stacked, the details of the unweathered surfaces and complete sections are preserved. Two types of vesicle patterns may be identified in these sections: (1) sections in which vesicles are distributed from top to bottom decreasing in abundance and attaining maximum sizes up to 1 cm just below the center of the sections, and (2) sections in which there is a upper vesicular zone in which vesicles decrease in abundance and increase in size; downward toward a central vesicle-free interior zone, and a lower vesicular zone near the base, typically 0.3 m thick in which vesicles increase in abundance and decrease in size downward. Jointing correspondingly increases in spacing with depth, so that the largest eroded blocks tend to be derived from the interiors.

This pattern of vesicle zonation and jointing characterizes sections in pahoehoe lavas throughout the world (Crumpler et al., 1983; Aubele et al., 1988; Walker, 1989) and was in part originally defined from the AVF. The development of regular trends in vesicles such as those shown in Figure 5 are a result of the competition between vesicle growth through several mechanisms, primarily through bubble coalescence, and inward-solidification of the flows from the top and bottom so that the most interior vesicles are able to grow larger. The overall vesicularity (volume percent of vesicles) remains nearly constant and appears to be inherited at the time of eruption (Walker, 1989). The slight decline in vesicularity within the interior is predicted from ideal gas law behavior of gases within vesicles and reflects the steady increase in hydrostatic pressure in the interior (Walker, 1989; Cashman and Kauahikaua, 1997; Crumpler et al., 1999).

An argument has been made that vesicle-free interior zones like that noted above in the earlier lavas (unit 1 of Kelley and Kudo, 1978) represent increased pressures over hydrostatic within the interior during lava inflation, a characteristic of some thin lava sheets (Hon et al., 1994). Inflated patterns common in unit 1 are interesting in that inflation of flows may be responsible for streamlined tumuli such as those distributed over the surface of Rinconada Point on the older surfaces. Subsequent deflation left behind local pillars and tumuli that were subsequently engulfed and surrounded either by an overlying flow unit or continued movement of the initially inflated flow.

It is on large and deeply varnished blocks detached from the lower part of the upper vesicular zone and vesicle-free interior that most petroglyphs occur because these present the smoothest, flattest, and largest surfaces, although the orthogonal edges of many large joint blocks were areas of artistic expression as well.

Later flows spreading outward near the fissure are more digitate and somewhat thicker. At least two flows distinctly puddled on the western side of the fissure after it had developed most of the relief observed today and were probably emplaced late in the eruption. At Vulcan, a flow emerged from the western edge of a late crater, and temporarily ponded near the exit from the breach (Fig. 6) before flowing west and north down the local relief of the fissure to the relatively flat terrain beyond. Where the flow moved onto the flat terrain, the width changed substantially, temporarily puddling at the foot of the fissure's slope as a perched lava pond. Another smaller and less voluminous lobe flowed westward from Black cone and is now preserved as a small ridge. This observation is useful in that the width of puddled or perched lava ponds depend critically on the volume flux, which will be estimated below based on the flow dimensions.

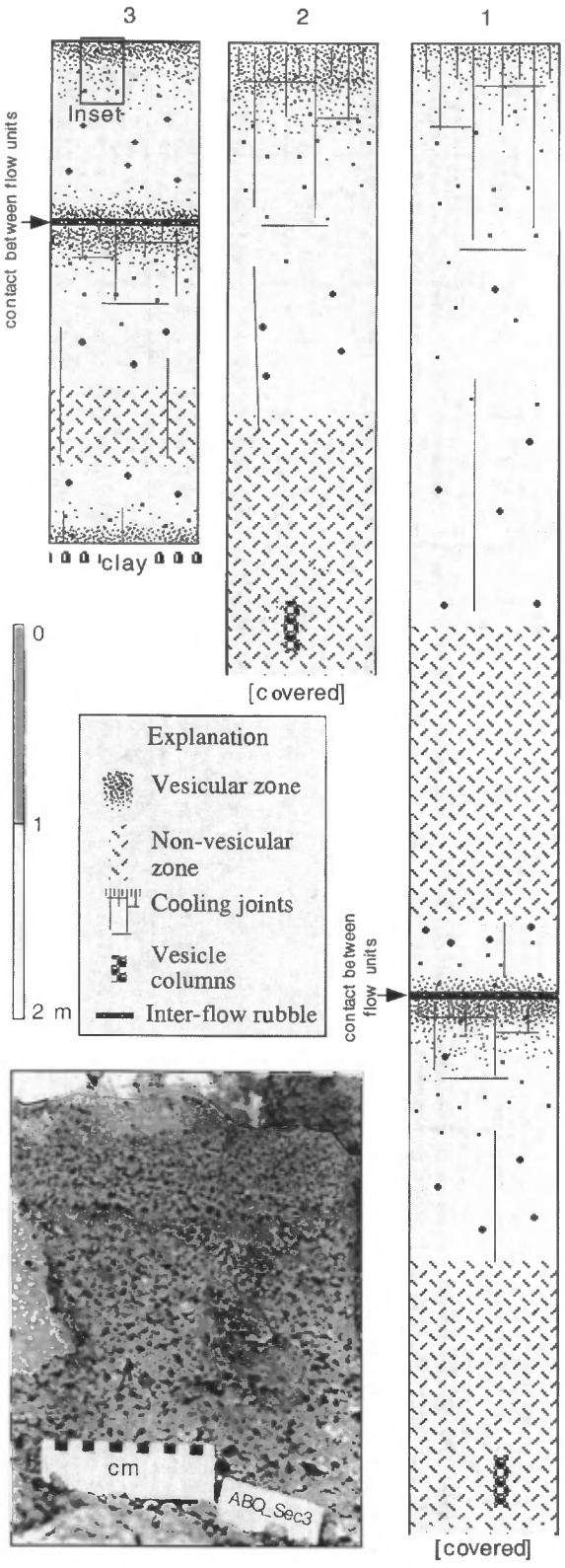

FIGURE 5. Measured lava sections from the eastern escarpment near Paradise Hills and Petroglyph National Monument showing characteristic vesicle zonation of flow units. Well-developed vesicular zones such as these are diagnostic of pahoehoe lava flows. Vesicle-free zones are interpreted to result from lava inflation and corresponding disturbance of gas-law behavior of depth-dependent vesicularity (volume per cent of vesicles) trend due to corresponding overpressures. Inset shows upper 33 cm of the upper flow unit in section 3, and illustrates the downward increase in vesicle average diameters and downward decrease in vesicle number density.

ASCENT AND EMPLACEMENT PROCESSES

Fissure eruptions similar to the AVF are physical evidence for the ascension of magma along tensile fractures as dikes that intersect the surface. There are few better examples of long fissure eruptions in the Southwest. The rarity of well-developed fissure eruptions, given the abundance of normal faulting and regional extension associated with mid to late Cenozoic tectonism in the western U.S., is notable. Conditions of tension along the Ceja Mesa may have been more favorable for large diking events and enabled magma ascent along long fissures for several reasons. First, the Ceja Mesa lies along the arch-like crest of the broad structural flexure beginning on the western side of the Rio Puerco and tilted down to the east. As a result, the upper crust along the divide between the Rio Puerco and Rio Grande has been under relative tension throughout its formation. Second, the relatively shallow depth to the asthenosphere, estimated at as little as 40 km beneath the central axis of the Rio Grande rift (Olsen et al., 1979), afforded ample opportunity for the propagation of cracks both downward from strong deviatoric tension in the upper lithosphere, and upward from magmatic overpressures associated with emplacement of melts in the shallow mantle. Third, the relatively strong tensile stress field, in combination with the direct access to the melt reservoir, enabled relatively greater dike widths and corresponding greater dike length.

Inferences from controls on dike depth, shape, and width

Understanding the geometry of the dike responsible for the AVF is useful both for interpreting the history of the AVF eruptions and for predictions about potential future eruptions from magma bodies within the Rio Grande rift. The length, width, and height of a dike strongly influence the character of the eruption when it intersects the surface. Dikes may propagate to the surface either by growing from the melt source region until they extend to the surface or by detaching from the melt source and ascending as separate bodies in thin cracks. The three-dimensional shape of dikes that ultimately influences the length, width, and volume flux of a fissure is tightly controlled by the mechanical properties of the lithosphere and upper crust. An estimate of the physical dimensions of the dike underlying the AVF is desirable in that it may constrain the depth from which the magmas propagated. Some estimates of dike dimension may be determined from the equation of state for dikes modeled as pressure-filled cracks (Weertman, 1971; Pollard and Muller, 1976; Gudmundsson, 1984), and the corresponding

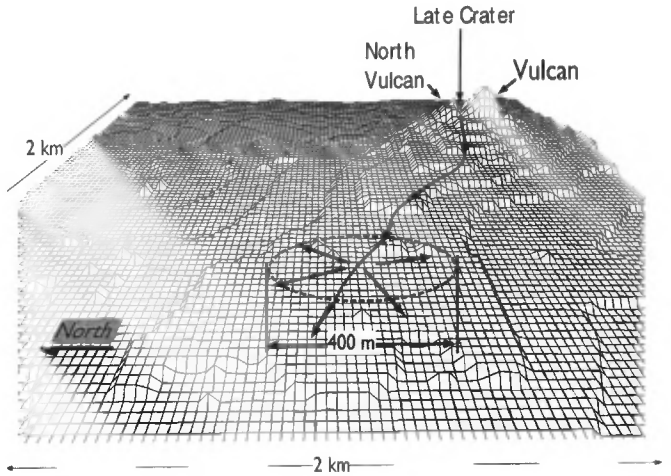

FIGURE 6. Eastward-directed perspective view based on 1:24,000-scale digital relief data. A 400-m wide, ponded lava flow lobe occurs northwest of Vulcan. Anomalously large late flows similar to this are common in many small volcanic centers throughout the Southwest. It is argued in the text that such flows reflect high effusion rates resulting from unusually high driving pressures during the final stages of eruption. In Hawaiian volcanoes, this type of event might have marked clearing of the vent region in preparation for the beginning of a new phase of eruption fed from the summit reservoir. In the simpler, closed geometry of the dike feeding AVF, this was a terminal event.

models of dike three-dimensional shapes (Maaløe, 1987). The elastic model, although imprecise, is a useful starting point and relates the pressure p required to maintain a dike of width w and length L in country rocks, $\{w/L\} \approx \Delta p/\{\mu/[2(1-v)]\}$, where v is Poissons ratio and μ, the shear modulus. As the shear modulus increases, the dike width decreases for a given internal pressure and length. Δp may be equated with the driving pressures $\Delta p = p_m - \sigma_3$, in which Pm is the excess magmatic pressure over the lithostatic load and σ_3 is the least principal stress, or remote stress magnitude. The magma pressure p_m is a function of several variables, including viscous, elastic, and material fracture strength properties (Reiches and Fink, 1988). These properties are important if the details of the local stress field and country rock stress state are to be considered. The driving pressure necessary to sustain flow up the dike from the melt reservoir follows from the conditions under which dike propagation initiates, $p + pm = \sigma_3 + T$, which is of the order of the tensile strength (T) of crustal materials typical in most crustal materials at scales of several kilometers. A corresponding value for Δp is of the order of 10 MPa (Maaløe, 1987) or less (<4 MPa, Pollard 1987; 1–4 MPa, Einarsson and Brandsdottir, 1980), and μ, 20 GPa and v, 0.1. Applying these values to the AVF fissure, a dike several meters wide (± 8 m) is implied for a dike 8 km long.

The actual fissure is segmented in a 2-km-long en-echelon arrangement, so the relevant dike length where the dike interacted with the surface is 2 km. This implies (from the above relations) an upper dike feeding the actual surface fissure less than 2 m wide. Using the results of Maaløe (1987) and Secor and Pollard (1975) relating height, width, and length of magma filled fractures in the crust, the maximum height of the parental dike for the AVF is on the order of 10 km, and the dikes associated with the en echelon surface fissures on the order of 2 km. The classic dislocation theory of dike geometry of Weertman (1971) provide similar estimates for the height of a magma filled crack with the given length. Assuming a simple model in which a larger dike relays upward to smaller segmented dikes and combining the lengths, yields a maximum vertical extent on the order of 12 km. These results predict that even the combined vertical length of the dikes feeding the AVF is less than the shallowest estimated potential melt source depths. A depth of 40 km (Olsen et al., 1979) is estimated for the upper mantle melt source depth beneath the central axis of the Rio Grande rift. The implication is that the dikes do not propagate all the way from a shallow subrift asthenosphere, but are detached and must have propagated from mid-crustal depths, perhaps a crustal reservoir. Alternatively, continuing the stacking model above, the parent dike could be fed in turn from a much larger dike extending for a significant length of the Ceja Mesa and 10–20-km deep.

One difficulty with these results is that they assume that the fissure length directly measures the length of the dike. The fissure length in reality can only be taken as a minimum estimate. This follows from the fact that only a small uppermost portion of the dike, which is generally modeled as parabolic in longitudinal section, is likely to intersect the surface. Thus the actual dike length may be longer by several times the fissure length. If the dike extended for a significant fraction of the length of the Albuquerque-Belen basin, then direct ascent from the asthenosphere may have been possible.

We can speculate that the distinctive Hawaiian eruptive style of the AVF could have arisen from unusually large remote stress (less principal stress component, σ_3) characteristic at the time of the eruption. As noted above, tension along the Ceja Mesa may have been unusually large during the late extensional history of the basin.

Ascent from mid-crustal level

Ascent from mid-crustal depths appears to be a common characteristic of many magmatic systems in the western United States. Several origins have been proposed for this characteristic, including rheological barriers to ascent, stress barriers, and buoyancy considerations. Rheological mechanisms fail because at the strain rates associated with magma ascent, crustal rocks are relatively weak and easily fractured. Loss of buoyancy by mafic magmas at mid-crustal depths (Glazner and Ussler, 1988) is consistent with the systematics of magma driving pressure outlined above and the observed density structure of the crust from seismic observations. Once trapped, further ascent cannot occur until sufficient driving pressure is attained to continue upward.

Several mechanisms exist whereby a magma initially trapped at mid-crustal depths can ascend, including volatile exsolution and vesiculation, accumulation of elastic strain energy from injection of magmas from below (Wadge, 1987), and differentiation of the magma in the upper levels to less mafic and dense phases. Alternately, dike propagation may occur if the least principal stress component decreases upward significantly due to remote (tectonic) stresses operating in the upper crust. In addition, an unusually large and more equant (as opposed to tabular or sheet-like) reservoir can attain driving pressures sufficient to propagate a dike upward regardless of the dike geometry, buoyancy, or state of stress in the overburden (Gudmundsson, 1988). It is clear that knowledge of dike propagation is incomplete, and the above models must be viewed as exploratory. Even the details of existing models remain to be worked out, but it is clear that many differences in the morphology of volcanic vents in the Southwest can arise from variations in the equilibrium and disequilibrium between rates of magma accumulation, volatile content, exsolution rate, and prevailing tectonic stresses. Corresponding differences in the eruption history will result from these variations so that magmas of otherwise similar petrologic characteristics may generate distinctly different landforms. These factors point to a broad outline of areas for future research into the origins of disparate eruption characteristics and morphologies in basaltic volcanoes.

Interaction with upper crust

The factors that may cause a dike to propagate from 12 km and segment in the last 2 km with a slightly different orientation relate to the details of the structure and state of stress in the upper crust. The explanation relies on an analysis of the Griffith-Coloumb yield criteria, and was explored by Reiches and Fink (1988) for the emplacement of the segmented dikes beneath the Inyo domes. Some of their results are applicable to understanding the segmented characteristic of the AVF fissure eruption.

In a homogeneous lithosphere, dikes will propagate upward along a single plane. Departures from this plane arise from variations in the mode of fracturing in the crust just ahead of the upward propagating dike tip and from upward gradients in stress from lithostatic to significant tectonic stress. Magma tends to invade tensile fractures at relatively great depths and at shallow depths may favor injection along shear fractures under some conditions of regional tectonic stress (Reiches and Fink, 1988). The transition can result in deflection from a single plane. Under these conditions, a large parent dike will segment along several en echelon fractures in the upper end. Significant vertical discontinuity in rock properties and regional tectonic stresses are two factors that may influence the transition in fracture modes. The former type of discontinuity is inherent at the boundary between deep crystalline Precambrian rocks to sedimentary rocks, including the Santa Fe Group at a depth of several kilometers. The orientation and scale of the en echelon arrangement of fissures no doubt carries some information about the stress regime in the Albuquerque basin at the time of eruption and is a useful area for future research. Whatever the exact influence, there are numerous opportunities for an upward propagating dike to segment according to differences in the mode of fracture and orientation of remote stresses.

Surface deformation (Fig. 7) associated with dilation above dike tips (Pollard, 1987; Mastin and Pollard, 1988) may provide additional information regarding the geometry of the underlying dike. Dilation of the dike walls is accommodated as displacements in the surface of up to 10% of the dike width for distances of up to ten times the dike width beyond the tip (Pollard, 1987) as a dike approaches a free surface. Empirical measurements of this influence from level line measurements in Iceland and Hawaii indicate total horizontal extension of up to 2/3 the dike width. One consequence of this is the prediction of graben-like fractures in the surface, the width and total strain of which are a function of width of the dike and depth to the dike tip (Mastin and Pollard,

1988; Head and Wilson, 1993). Using Mastin and Pollard's results, a total horizontal extension of up to 5 m is predicted in the near surface associated with a shallow parent dike underlying the AVF. Assuming a dip on bounding faults of 60°, a graben less than 4-m deep should result. The graben width reflects the distance between strain maxima which are strongly influenced by the depth to the dike tip. Based on the work of Mastin and Pollard (1988), an 8-m-wide dike at a depth of 2–4 km estimated for the parent dike above, would result in a graben width on the order of 2 km. Such a depression is consistent with the depressions and possible linear trough, discussed earlier, and interpreted as responsible for the anomalously thick lava section at Mesa Prieta on the southern end of the field. Unfortunately, there are no existing data for distinguishing between graben developed for simple tectonic reasons and graben arising from near surface deformation of a dike, so this origin for those structures remains speculative and circumstantial evidence for dike-induced deformation. More detailed mapping is appropriate in the future combined with geophysical methods in order to identify the details of the faulting and structures of the deep crust in this area.

Cone and vent emplacement

Some of the more revealing and better preserved characteristics of the Albuquerque volcanoes occur in the individual cones. Several questions may be addressed on the basis of the observed morphology and structure in these vents, including the origin of the separate cones from a long fissures, the origin of the secular changes in pyroclastic activity and eruption style during the history of the eruption, and the origin of differences in the local cone morphology.

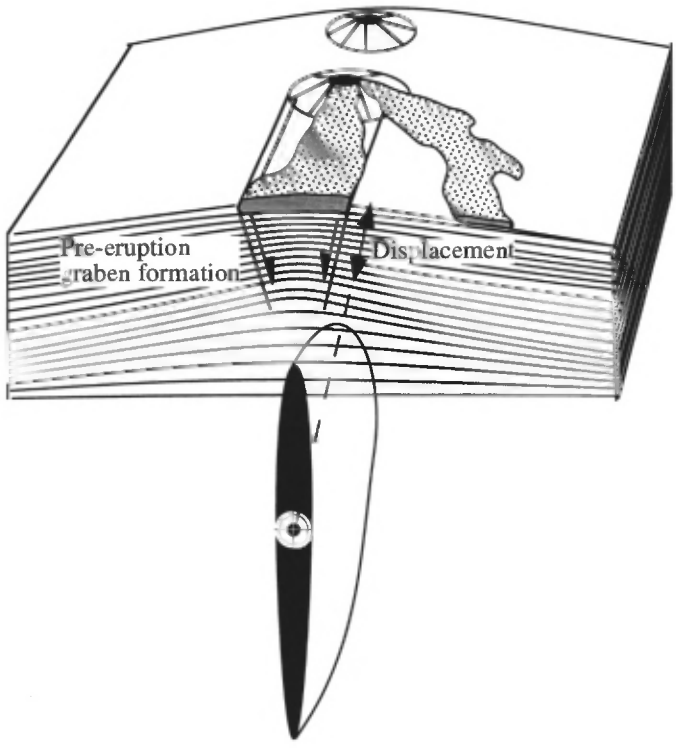

FIGURE 7. Illustration of predicted displacements along the free surface above a propagating dike tip. Graben and normal faults are observed to occur during shallow dike emplacement (Masten and Pollard, 1988) and should occur at sites of older eruptions. If the graben is wide and deep, lava flows and pyroclastic deposits from the earliest eruptions of the subsequent fissure will accumulate within the local depression and become substantially thicker than later deposits erupted onto more uniform surfaces.

Exit vent centralization

Steady eruption occurred as long as driving pressures could sustain the flow and appropriate thermal conditions were maintained to keep the dike from solidifying. The physical characteristics of spacing, size, and eruption style that resulted in the row of volcanoes along the AVF fissure reflect the fluid and thermal dynamics of early fissure flow. Bruce and Huppert (1989) have shown that for a fissure eruption, there is a critical dike width (~2 m) for any given fissure length in order for eruption to proceed. For dikes wider than this critical width, sustained flow may occur as long as there is a steady supply of magma from the source reservoir. For narrower dikes, eventual blockage will occur regardless of magma supply. The width is so critical that natural irregularities in the width of the fissure will cause some narrower areas of a fissure to close while wider segments will remain open and even grow in width due to melt-back of the walls as these remaining areas take up the continuing flux. The influence of irregularities in width are such that preferential areas of venting are predicted to become established over a matter of days after inception of the fissure eruption as narrower zones become quickly blocked. The dike width for the en echelon AVF fissures estimated earlier above, are within the range for this criterion of stability, thus enabling maintenance of the fissure. The principal vent areas now represented by cones thus emerged very quickly (days) in the history of the eruption.

Another consequence predicted by this model is the emergence of the relatively regular spacing of vents as a result of cross-flow along the dike in which initially wider segments of a dike pirates flow from adjoining narrower segments. The further restricted flux results in the reduction in advected heat flow, already lower in these segments, and "seals" their fate. Given the limited volume available for eruption and sensitivity to volume flux, cross-flow will be expressed as uniformly spaced exit areas. The emergence of preferred vent areas with regular spacing thus represents a type of "feed back" phenomenon frequently noted in discussions of heat and mass flux of volcanic systems.

Based on the differing overall morphologies and flank deposits of the vents, once the principal vents were established, their eruption histories diverged in detail while following similar overall trends in eruption associated with the secular changes in the relative content of gas and magma volume supply rates of the primary dike.

Inferences about the gas content from pyroclastic deposits

The secular changes from Hawaiian to Strombolian activity along the fissure are interpreted to reflect two variables: gas content and magma volume flux. Head and Wilson (1981, 1989) have shown from numerical and empirical studies, that the interaction of volume flux and gas content at a vent controls the dynamic structure of fire fountains, in particular the dispersal and optical opacity, and the rates of cooling of pyroclasts prior to deposition. It is the temperature upon landing and the rate of accumulation of pyroclasts that control the corresponding physical state of the final pyroclastic deposits, i.e., cinders versus spatter; ash versus rootless flows; and so on.

The poorly welded and brittle nature of the pyroclasts in the cinder pit at Vulcan imply relatively low opacity and high dispersal in the fire fountain when it was deposited, in contrast to the high opacity and strong fountain collimation that must have occurred during emplacement of most of the lava field volume. The change in style from dominantly effusive to pyroclastic is consistent with a relative increase in gas content or decrease in volume flux at the vent. A secular change in both can be understood in terms of the competition between rise rate of magma in the dike feeding the fissure and ascent rate of gases in the magma. During stages of high-volume flux, volatiles emerge trapped with the magma. If the volatile content is high, in combination with high volume flux, optically thick, well-collimated fire fountaining result, individual pyroclasts are poorly cooled on landing, and rootless flows and lava streams result. During later stages of ascent, as the driv-

ing pressure, rise speed of the magma, and corresponding volume flux falls, the emerging magma transitions to Strombolian activity (Parfitt and Wilson, 1995), the fountain less collimated, and individual clast are cooler on landing. This results in fluid "plops" spatter and local rootless flows. As the volume flux falls further, the dispersal is greater, the fountain optically thin, and clast strongly cooled on landing. The result is fragmental scoria and ash. As the later-arriving magma batches may have been relatively de-volitalized, the trend toward relatively gas-rich, well-dispersed fountain structure reversed towards gas-poor, low-volume flux eruptions. The result was development of significant spatter and rootless flows characterizing the outer surfaces of most of the cones. As the driving pressure and volume of magma in the dike dropped to near-terminal values, volatiles once again were able to build. However, by this time the upper portions of the dike, particularly that within the cones had become blocked with cooler magmas, and sporadic, often violent eruptions occurred. Development of excessive overpressures could have been responsible for the significant late swelling and the explosions that occurred on several of the cones, including the explosion that disrupted the north flank of Vulcan.

Radial cracks and detached sectors at Vulcan and JA cone imply possible extension of the cone flanks. One reason why the degree of deformation appears unusual may be the relatively small size of the cones in relation to late near surface magma ejections. Dilation overlying a large dike on the order of the size of the conduit which must have fed the individual cones (5 m) could significantly inflate the cones. Instantaneous instability, aided by local-scale seismic accelerations during terminal activity, could further exacerbate the instability of the still-plastic lavas on an already steep slope.

The large flow lobe that ponded on the west base of Vulcan and Black Cone probably developed during a late, short period of high magma flux when driving pressures had been elevated by accumulation of volatiles in the upper dike. Following the clearing of the upper magma pathways by the last explosions, this enabled extrusion of remaining magmas in a large effusion event characterized by increased magma flux compared with that occurring throughout most of the waning stages of the eruption. On the basis of the stratigraphic relationships of the differing deposits, the pathway during the eruption in gas content versus volume flux space may be inferred from this model (Fig. 8). Refinement of the methodology used in plotting this path may be important in characterizing physical processes in small volcanic systems elsewhere in the Southwest.

In summary, the Hawaiian style of eruption that characterized the AVF represents a balance between the rise rate of entrained bubbles and volume flux of magma ascending in the dike. The resulting eruption is characterized by the steady discharge of magma in which the melt is disrupted at or near the surface by gases in the magmas. The gas content and disruption is such that the size of individual pyroclasts are relatively large and are not entrained in the convecting column above the vents. Instead, they fall back to the surface to contribute to rootless flows and steep accumulations of spatter. The Strombolian style typifying the development of the principal cones occurs when the rise rate of bubbles exceeds the magma rise rate. The change to dominantly pyroclastic activity in the AVF marked the transition in volume rate below a critical value necessary for optically opaque fire fountains. The resulting eruptions were characterized by staccato explosions at the vent and strong disruption of pyroclasts.

Lava flow emplacement

The pattern and magnitude of drainages graded to the ancestral Rio Grande as preserved in the lava flows of the AVF imply gradients much like those today, despite the fact that the surface has been incised from 50 to 60 m relative to the basalt. Blocks of the lava flows do not occur commonly beyond the base of the slopes leading up to the lava cliffs, so it is likely that back-wasting of the margins of the field has not been extensive. The overall shape and pattern of flowage away from the fissure vents provide a measure of shape and orientation of drainages during the eruption.

Inferences about volume eruption rate from lava flows

The maximum preserved lava flow length in the AVF is nearly 9 km and is attained by the lower stratigraphic units now making up the easternmost edges of the field exposed along the Petroglyph National Monument. This must be considered a minimum length estimate because the original extent of the longest flows prior to back-wasting of the distal parts of the flow field is unknown. Upper stratigraphic units within the field that were erupted from one or more of the principal

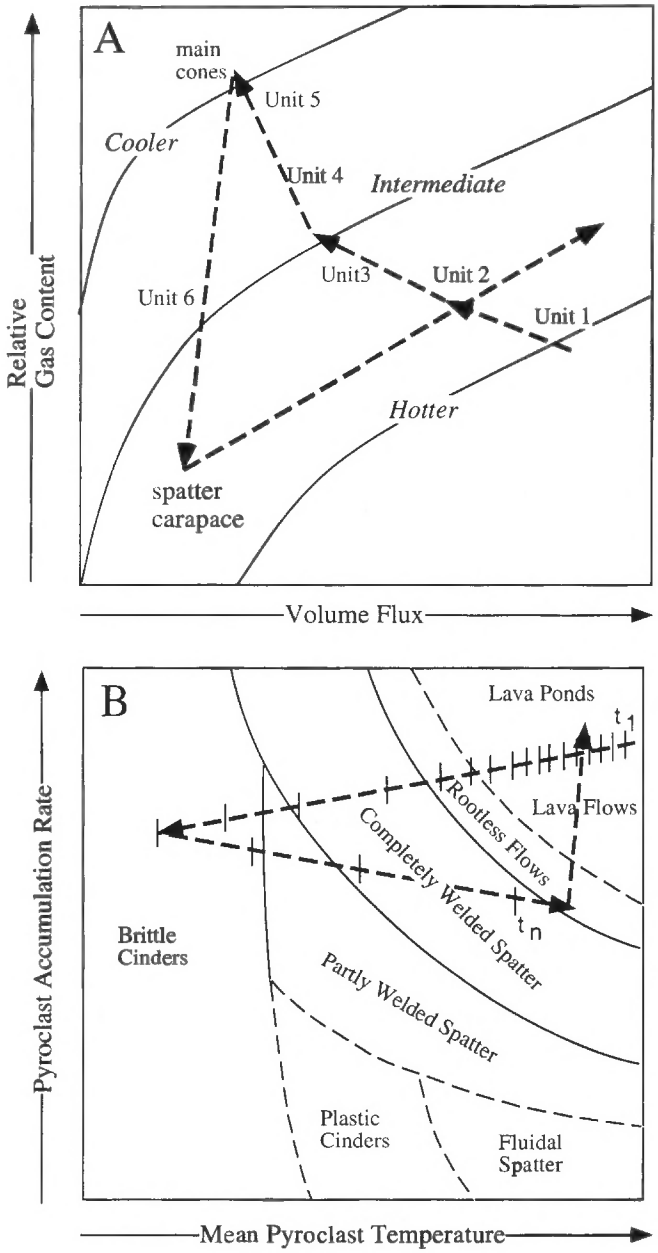

FIGURE 8. Probable pathway in time (indicated by direction of arrows) of gas content, volume flux, eruption characteristics, and character of corresponding pyroclastic eruption deposits for the AVF. Estimate is based on semi-quantitative model of the influence of volume flux and gas content (Head and Wilson, 1989) and models of the dynamics of two-phase flow in typical vents (Wilson and Head, 1981). **A**, The long-term trend was toward decreasing volume flux and increasing gas content. The actual pathway was probably more jagged with frequent excursions back and forth following short-term variations and pauses in flux at the fissure. **B**, The corresponding pyroclastic deposits evolved with time toward cooler and more brittle cinders until declining gas concentration during terminal eruption reversed the trend resulting in thick accumulations of spatter and flud agglomerate.

vents measure considerably less than this length (<1–2 km).

Quantitative estimates of actual values of volume flux that these differences in flow length and volume represent may be made on the basis of current understanding of the factors controlling lava flow lengths (Pinkerton and Wilson, 1994). Once initiated, the maximum length that lava flows of otherwise similar mechanical and thermal characteristics can attain will depend on the availability of a continued supply of lava from the vent, in which case the length is thermally limited. Otherwise the flow is volume-limited and runs out of supply before attaining its maximum theoretical length. For the thermally limited case, it has been argued that the length depends on the dimensionless Gratz number (Hulme and Fielder, 1977; Pinkerton and Wilson, 1994; Wilson and Head, 1994), which is the square of the ratio of the thickness of the flow to the distance that thermal cooling would have penetrated since the flow left the vent, and is given by

$$Gz = d^2\varepsilon/\kappa\, t = \psi^2\, f\, d/(\kappa\, w\, L),$$

where k is the thermal diffusivity, d the average flow thickness, w is the width of the channel in which lava flows, L is the flow length, ψ is a geometric parameter (for most flows equal to ~2), and f is the volume effusion rate (flux at the vent). Flows are observed to cease movement when the Gratz number reaches a critical value, Gz_C ~300, which sets the left side of the above expression. Considering the rheology of lavas as Bingham plastics, this can then be solved for the maximum length attainable in the thermally-limited case, L_{max} (Pinkerton and Wilson, 1994),

$$L_{max} = [1.34/(\kappa Gzc)](T/\eta)^{2/11} f^{9/11}[T/(\rho g)]^{6/11}\sin^{3/11}\alpha.$$

Substituting observed values for the variables from the AVF lava flows and using allowable estimates of diffusivity $\kappa(10^{-6}m^2s^{-1})$, yield strength T (2000 Pa), plastic viscosity η(30 Pa s^{-1}), density ρ (2000 kg m^{-3}), and slope α (as appropriate for each flow), the observed lengths represent a minimum flux (f) from 0.3 to 15 m^3s^{-1} (Table 1). The principal measurement are the lengths of several representative maximum length flow lobes from each stratigraphic unit. Within each stratigraphic unit there are shorter lobes that may be identified, so these effusion estimates are maxima for each stratigraphic unit.

The flux cast in terms of the approximate stratigraphic unit 1, 2, 3, 4, and 5 time (of Kelley and Kudo, 1978) (Fig. 9) implies decay in effusion rates over the fissure eruption duration, a characteristic of eruptions from isolated reservoirs in general. In the case of the AVF, the reservoir is the parental dike, and the decay probably follows from relaxation of elastic stress in the surrounding deformed crustal rocks after initiation of eruptions (Wadge, 1981).

Table 1. Measured lava flow lengths, and slopes, and estimated volume effusion rates.

Flow unit	Length/km	Slope/°	Flux (f)/m^3s^{-1}
1	8.7	1.0	15.2
1	8.4	1.0	14.3
1	4.8	1.8	6.1
1	6.0	1.5	8.4
1	4.3	2.0	5.2
2	8.1	1.0	13.9
2	3.9	1.6	4.9
2	5.2	1.1	7.7
2	2.6	2.0	2.7
3	3.4	1.6	4.2
3	3.2	1.6	3.9
3	3.4	1.8	3.9
3	4.0	1.7	4.9
3	4.5	1.6	5.9
3	2.1	2.5	2.0
4	1.6	3.3	1.3
4	2.1	2.5	2.0
4	1.5	3.0	1.2
4	1.8	2.5	1.6
4	1.0	4.5	0.6
5	0.6	4.1	0.4
5	0.5	5.4	0.3
5	0.6	4.1	0.4
5	0.5	4.9	0.3

An additional measure of the flux (f) can be obtained from the observation that some flows ponded on the western slopes of the fissure at Vulcan cone (Fig. 6). Wilson and Parfitt (1993) noted the extreme dependence of flow length and width on slope and flux. They therefore defined the lateral dimension of perched lava ponds (**X**) as a function of the change in slope (α) upstream from the local area of ponding and the flux (f_C) into the pond during growth such that

$$\mathbf{X} = \{f_C{}^4\xi\eta/[(5.8 \times 10^6)\,\pi^4\kappa^3\rho g \sin\alpha\}^{1/7}$$

where ξ is a geometric parameter related to the hydraulic radius of the flow. For the lava flow ponded on the west slopes of the fissure at Vulcan cone, ξ = 3. For the example here, the value of slope, α, is assumed to be that at the foot of the western lower flanks of Vulcan (0.25°). The calculation is not sensitive to h, so we may safely assume a value equivalent to Hawaiian tholeiites (30 Pa s^{-1}) at their eruption temperatures. Because of the fourth power-dependence on flux (f_C), the exact dimensions of the pond are not critical, which in this case is **X** = 400 m. The flux for the Vulcan ponded flow lobe is estimated accordingly at f_C = 100 m^3s^{-1}. This is an order of magnitude greater than even the opening stages of the eruption. A somewhat similar flow on the western side of Black Cone appears to have developed near the same time. An estimate of flux from the geometry of the Black Cone ponded flow lobe cannot be made, as it appears that significant spreading did not occur. This suggests that this particular flow was volume-limited and thus did not attain the maximum flow-out typical of mature perched lava ponds.

The order of magnitude greater effusion for the late ponded flow hints at the violence of this last event. Similar massive and ponded flows are known from other scoria cones in the Southwest (e.g., Crumpler et al., 1994). These usually accompany catastrophic lateral movement and collapse of large sectors of cinder cone flanks. Although the details leading up to the event at Vulcan cone differ from many of these examples, the process is fundamentally similar. During the waning stages of

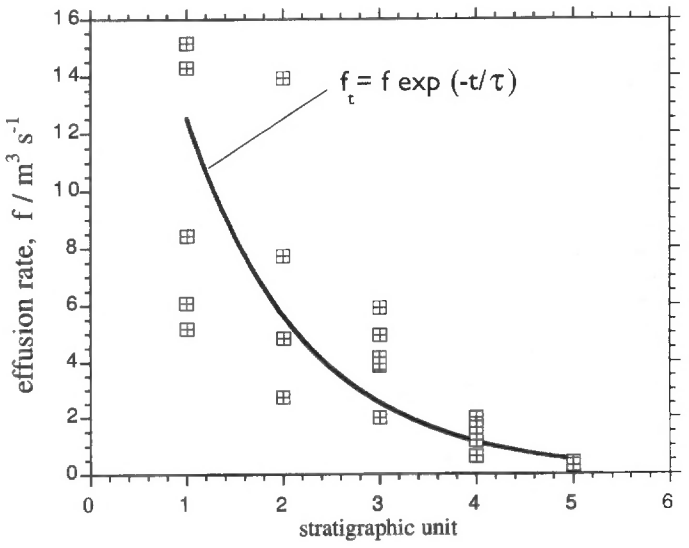

FIGURE 9. Magma volume flux (boxes) at approximate 1, 2, 3, 4, and 5 stratigraphic unit time (of Kelley and Kudo, 1978) estimated from the lengths of individual representative lava flow lobes from each stratigraphic unit. Calculation assumes that flows are thermally limited, i.e., follow Gratz behavior in which flows cease movement when Gz ~300. The steady decline in volume effusion rates from an initial value (f) is fitted with an inverse exponential expression. The decline in effusion with time (t) during eruption from a closed reservoir undergoing elastic stress relaxation of surrounding crustal rocks (Wadge, 1981) is an example of such a relation in which $\tau = (12\eta h V_T)/(K w^3 L)$; η = magma viscosity; h = dike height; V_T = volume of deformed crustal rocks; K = bulk modulus of crustal rocks; w = dike width; and L = dike length.

eruptions driving pressures are low, perhaps because the batches of magma within the upper parts of the reservoir or dike that had accumulated the most volatiles are nearly exhausted. As driving pressures are low, the vent is susceptible to blockage as the pressure drops below that necessary to overcome the combined yield strength of debris and cooled magmas in the upper part of the conduit or dike. If sufficient magma remains in the reservoir or deeper levels of the dike, effusion can continue only when volatiles accumulate and an increase in driving pressures is attained sufficient to overcome the yield strength of the blocking materials.

The volume effusion rates estimated for the AVF are typical of Hawaiian fissure eruptions. Unlike Hawaiian eruptions in which the feeding dike is periodically re-supplied by a larger reservoir (Parfitt and Wilson, 1994), the AVF was supplied by a single deep dike held open against elastic stresses in the crust by contained magmas. As stresses were relaxed with continued eruption, the result was a much simpler monotonically decreasing volume rate with time consistent with a closed reservoir behavior. The fact that the mechanics of eruption in many continental volcanic systems are, like the AVF, simpler in this respect, and much more easily understood, in addition to being more widespread, illustrates the importance of studies of basaltic volcanoes other than active oceanic shield volcanoes.

ACKNOWLEDGMENTS

Elizabeth Parfitt, Leeds University, U.K.; Eric Grosfils, Pomona College, California; and Jayne Aubele, New Mexico Museum of Natural History and Science graciously provided insightful and constructive volcanological reviews on short notice.

REFERENCES

Aoki, K. and Kudo, A. M., 1976, Major element variations of late Cenozoic basalts of New Mexico: New Mexico Geological Society, Special Publication 5, p. 82–88.

Aubele, J. A., Crumpler, L. S. and Elston, W. E., 1988, Vesicle zonation and vertical structure of basalt flows: Journal of Volcanology and Geothermal Research, v.35, p. 349–374.

Bachman, G. O. and Mehnert, H. H., 1978, New K-Ar dates and the late Pliocene to Holocene geomorphic history of the central Rio Grande region, New Mexico: Geological Society of America Bulletin, v. 89, 283–292.

Baldridge, W. S., 1979, Petrology and petrogenesis of Plio–Pleistocene basaltic rocks from the central Rio Grande Rift, New Mexico, and their relation to rift structure; *in* Reiker, R. E., ed., Rio Grande rift: Tectonics and magmatism: American Geophysical Union, Washington, D.C., p. 323–353.

Bruce, P. M. and Huppert, H. E., 1989, Thermal controls of basaltic fissure eruptions: Nature, v. 342, p. 665–667.

Cashman, K. V. and Kauahikaua, J. P., 1997, Reevaluation of vesicle distribution in basaltic lava flows: Geology, v. 25, p. 419–422.

Crumpler, L. S., Aubele, J. A. and Elston, W. E., 1983, Basalt flow vertical structure and vesicle zonation: Geological Society of America, Abstracts with Programs, v. 15, p. 419.

Crumpler, L. S., Aubele, J. A. and Condit, C. D., 1994, Volcanoes and neotectonic characteristics of the Springerville volcanic field, Arizona: New Mexico Geological Society, Guidebook 47, p. 147–164.

Crumpler, L. S., Cashman, K. V. and Schultz, R., 1999, Vesicles: A fundamental characteristic of planetary surface rocks: 30th Lunar and Planetary Science Conference Abstracts, in press.

Einarsson, P. and Brandsdottir, B., 1980, Seismological evidence for lateral magma intrusion during the July 1978 deflation of Krafla volcano in NE Iceland: Journal of Geophysics, v. 47, p. 160–165.

Glazner, A. F. and Ussler III, W., 1988, Trapping of magma at midcrustal density discontinuities: Geophysical Research Letters, v. 15, p. 673–675.

Gudmundsson, A., 1984, Formation of dykes, feeder-dykes, and the intrusion of dykes from magma chambers: Bulletin of Volcanology, v. 47, p. 537–550.

Gudmundsson, A., 1988, Effect of tensile stress concentration around magma chambers on intrusion and extrusion frequences: Journal of Volcanology and Geothermal Research, v. 35, p. 179–194.

Head, J. W. and Wilson, L., 1981, Ascent and eruption of basaltic magmas on Earth and Moon: Journal of Geophysical Research, v. 86, p. 2971–3001.

Head, J. W. and Wilson, L., 1989, Basaltic pyroclastic eruptions: influence of gas-release patterns and volume fluxes on fountain structure, and formation of cinder cones, spatter cones, rootless flows, lava ponds, and lava flows: Journal of Volcanology and Geothermal Research, v. 37, p. 261–271.

Head, J. W. and Wilson, L., 1993, Lunar graben formation due to near-surface deformation accompanying dike emplacement: Planetary and Space Science, v. 41, p. 719–727

Holmes, R. F., 1987, Significance of agglutinate mounds on lava flows associated with monogenetic cones: an example at Sunset Crater, northern Arizona: Geological Society of America Bulletin, v. 99, p. 319–324.

Hon, K., Kauahihaua, J., Denlinger, R. and Mackay, K., 1994, Emplacement and inflation of pahoehoe sheet flows: observations and measurements of active lava flows on Kilauea volcano, Hawaii: Geological Society of America Bulletin, v. 106, p. 351–370.

Hulme, G. and Fielder, G., 1977, Effusion rates and rheology of lunar lavas: Philosophical Transactions of the Royal Society of London, Series A, v. 285, p. 227–234.

Kelley, V. C. and Kudo, A. M., 1978, Volcanoes and related basalts of Albuquerque-Belen basin, New Mexico: New Mexico Bureau of Mines and Mineral Resources, Circular 156, 31 p.

Kelley, V. C., 1977, Geology of Albuquerque basin, New Mexico: New Mexico Bureau of Mines and Mineral Resources, Memoir 33, 59 p.

Kelley, V. C., 1982, Albuquerque: Its mountains, valley, water, and volcanoes: New Mexico Bureau of Mines and Mineral Resources, Scenic Trips to the Geologic Past, No. 9, p. 29–35, p. 98–104.

Kudo, A. M., Kelley, V. C., Damon, P. E. and Shafiquallah, M., 1977, K-Ar ages of basalts at Canjilon Hill, Isleta Volcano, and Cat Hills volcanic field, Albuquerque-Belen basin, central New Mexico: Isochron/West, n. 18, p. 15–16.

Kudo, A. M., 1982, Rift volcanics of the Albuquerque basin: Overview with some new data: New Mexico Geological Society, Guidebook 33, p. 285–289.

Maaløe, S., 1987, The generation and shape of feeder dykes from mantle sources: Contributions to Mineralogy and Petrology, v. 96, p. 47–55.

Mastin, L. G. and Pollard, D. D., 1988, Surface deformation and shallow dike intrusion at Inyo Craters, Long Valley, Califomia. Journal of Geophysical Research, v. 93, p. 13,221–13,235.

Olsen, K. H., Keller, G. R. and Stewart, J. N., 1979, Crustal structure along the Rio Grande Rift from seismic refraction profiles; *in* Reiker, R. E., ed., Rio Grande rift: Tectonics and magmatism: American Geophysical Union, Washington, D.C., p. 127–144.

Parfitt, E. A. and Wilson, L., 1993, The formation of perched lava ponds on basaltic volcanoes: the influence of flow geometry on cooling-limited lava flow lengths: Journal of Volcanology and Geothermal Research, v. 56, p. 113–123.

Parfitt, E. A. and Wilson, L., 1994, The 1983-86 Pu'u'O eruption of Kilauea volcano, Hawaii: A study of dike geometry and eruption mechanisms for a long-lived eruption: Journal of Volcanology and Geothermal Research, v. 59, p. 179–205.

Peale, D. W., Chen, J. H., Wasserburg, G. J. and Papanastassiou, D. A., 1996, ^{238}U-^{230}Th dating of a geomagnetic excursion in Quaternary basalts of the Albuquerque volcanoes field, New Mexico (USA): Geophysical Research Letters, v. 23, p. 2271–2274.

Perry, F. V., Baldridge, W. S. and DePaolo, D. J., 1987, Role of asthenosphere and lithosphere in the genesis of late Cenozoic basaltic rocks from the Rio Grande rift and adjacent regions of the southwestern United States: Journal of Geophysical Research, v. 92, p. 9193–9213.

Pinkerton, H. and Wilson, L., 1994, Factors controlling channel-fed lava flows: Bulletin of Volcanology, v. 56, p. 108–120.

Pollard, D. D. and Muller, O. H, 1976, The effects of gradients in regional stress and magma pressure on the form of sheet intrusions in cross section: Journal of Geophysical Research, v. 81, p. 975–984.

Pollard, D. D., 1987, Elementary fracture mechanics applied to the structural interpretation of dykes: *in* Halls, H. C. and Fahrig, W., eds., Mafic dyke swarms: Toronto, Geological Association of Canada, Special Paper 34, p. 5–24.

Reiches, Z. and Fink, J., 1988, The mechanism of intrusion of the Inyo dike, Long Valley caldera, California: Journal of Geophysical Research, v. 93, p. 4321–4334.

Rhinehart, E. J., Sanford, A. R. and Ward, R. M., 1979, Geographic extent and shape of an extensive magma body at midcrustal depths in the Rio Grande rift near Socorro, New Mexico; *in* Reiker, R. E., ed., Rio Grande rift: Tectonics and magmatism: American Geophysical Union, Washington D.C., p. 237–252.

Secor, D. T. and Pollard, D. D., 1975, On the stability of open hydraulic fractures in the Earth's crust: Geophysical Research Letters, v. 2, p. 510–513.

Simmons, M, 1982, Albuquerque: A narrative history: University of New Mexico Press, Albuquerque, p. 8.

Tait, S., Jaupart, C. and Vergniolle, S., 1989, Pressure, gas content and eruption

periodicity of a shallow, crystallizing magma chamber: Earth and Planetary Science Letters, v. 92, p. 107–123.

Wadge, G., 1981, The variation in magma discharge during basaltic eruptions: Journal of Volcanology and Geothermal Research, v.11, p. 139–168.

Walker, G. P. L., 1989, Spongy pahoehoe in Hawaii: A study of vesicle-distribution patterns in basalt and their significance: Bulletin of Volcanology, v. 51, p. 199–209

Weertman, J., 1971, Theory of water-filled crevasses in glaciers applied to vertical magma transport beneath oceanic ridges: Journal of Geophysical Research, v. 76, p. 1171–1183.

Williams, H and McBirney, A. R., 1979, Volcanology: Freeman, Cooper, and Company, San Francisco, 397 p.

Wilson, L. and Head, J. W., 1994, Mars: Review and analysis of volcanic eruption theory and relationships to observed land forms: Reviews of Geophysics, v. 32, p. 221–264.

Wood, C. A.,1980, Morphometric evolution of cinder cones: Journal of Volcanology and Geothermal Research, v. 7, p. 387–413.

Wood, C. A., and Kienle, J., 1990, Volcanoes of North America: Cambridge University Press, Cambridge, p. 147–314.

Zimmerman, C. and Kudo, A. M., 1979, Geochemistry of andesites and related rocks, Rio Grande rift, New Mexico; *in* Reiker, R. E., ed., Rio Grande rift: Tectonics and magmatism: Washington, D.C., American Geophysical Union, p. 355–381.

Frank Kottlowski gives his impression of the "Great Stone Face" while keeping the sun off his neck on the the 1988 NMGS field trip to southwestern New Mexico. Do you think that Richard Chamberlin (right) has a toothache or does his stance represent total disbelief? (photograph courtesy of George Austin.)